OH_3^- and $O_2H_5^-$ double Rydberg anions: Predictions and comparisons with NH_4^- and $N_2H_7^-$

Junia Melin, and J. V. Ortiz

View Online   Export Citation

ARTICLES YOU MAY BE INTERESTED IN

OH$_3^-$ and O$_2$H$_5^-$ double Rydberg anions: Predictions and comparisons with NH$_4^-$ and N$_2$H$_7^-$

Junia Melin and J. V. Ortiz[a)]
Department of Chemistry and Biochemistry, Auburn University, Auburn, Alabama 36849-5312

A low barrier in the reaction pathway between the double Rydberg isomer of OH$_3^-$ and a hydride-water complex indicates that the former species is more difficult to isolate and characterize through anion photoelectron spectroscopy than the well known double Rydberg anion (DRA), tetrahedral NH$_4^-$. Electron propagator calculations of vertical electron detachment energies (VEDEs) and isosurface plots of the electron localization function disclose that the transition state's electronic structure more closely resembles that of the DRA than that of the hydride-water complex. Possible stabilization of the OH$_3^-$ DRA through hydrogen bonding or ion-dipole interactions is examined through calculations on O$_2$H$_5^-$ species. Three O$_2$H$_5^-$ minima with H$^-$(H$_2$O)$_2$, hydrogen-bridged, and DRA-molecule structures resemble previously discovered N$_2$H$_7^-$ species and have well separated VEDEs that may be observable in anion photoelectron spectra. © *2007 American Institute of Physics*. [DOI: 10.1063/1.2741558]

INTRODUCTION

In a double Rydberg anion, a closed-shell, molecular cation binds a pair of diffuse electrons.[1–4] The first example to be observed and characterized[1,5,6] was tetrahedral NH$_4^-$, a species whose existence was anticipated in computational studies.[7,8] The photoelectron spectrum of mass-selected NH$_4^-$ anions exhibits a dominant peak that was assigned to electron detachment from the anion of a hydride-ammonia complex.[9] However, at lower electron binding energy and with much lower intensity, certain features occur that were assigned by experimentalists to a tetrahedral species.[1,5,6] These conclusions were confirmed subsequently by *ab initio* predictions of a stable tetrahedral minimum with a positive adiabatic electron detachment energy.[10–13] In addition to the peaks that correspond to vertical transitions, features that correspond to electron detachment accompanied by vibrational excitation were assigned.[14] Accurate electron propagator calculations of electron binding energies have been an essential foundation of these assignments and their interpretation in terms of qualitative molecular orbital concepts.[3,4,10,13,15] In electron propagator calculations,[16] solutions of the quasiparticle form of the Dyson equation,

$$[\hat{f} + \hat{\Sigma}(\varepsilon_i)]\phi_i^{\text{Dyson}}(x) = \varepsilon_i \phi_i^{\text{Dyson}}(x), \qquad (1)$$

where $\hat{f}$ is the Fock operator and $\hat{\Sigma}(\varepsilon_i)$ is the energy-dependent, nonlocal, self-energy operator that describes orbital relaxation and electron correlation effects, yield electron binding energies (ε_i) and associated Dyson orbitals. The latter are related to the initial (N electron) and final ($N-1$ electron) states of photoelectron spectroscopy by

$$\phi_i^{\text{Dyson}}(x_1) = \sqrt{N} \int \Psi_N(x_1, x_2, x_3, \ldots, x_N)$$
$$\times \Psi_{i,N-1}^*(x_2, x_3, \ldots, x_N) dx_2 dx_3 \cdots dx_N, \qquad (2)$$

where x_k is the space-spin coordinate of electron k, and describe changes in electronic structure that accompany electron detachment. Dyson orbitals corresponding to the lowest vertical electron detachment energy of tetrahedral NH$_4^-$ have been obtained with various approximations for the self-energy operator. In all of these calculations, the Dyson orbitals have the following characteristics:

- they are totally symmetric under all symmetry operations;

- their largest amplitudes occur outside the hydrogen nuclei; and

- they have two radial nodes, one of which is close to the hydrogen nuclei.[3]

In the united atom limit, these Dyson orbitals correlate to the 3s orbital of Na$^-$. Geometry optimizations also have established that bond lengths in tetrahedral NH$_4^-$ are only slightly longer than those in the uncharged radical. These results imply that two electrons occupy a diffuse, nonbonding orbital that is delocalized on the periphery of an ammonium core and provide justification for the concept of a double Rydberg anion. The Dyson orbital for the lowest vertical electron detachment energy of the hydride-ammonia complex consists chiefly of s functions on the hydride nucleus.[10]

Subsequent experimental[14] and theoretical[15] reports have considered N$_n$H$_{3n+1}^-$ double Rydberg anions for $1 \leqslant n \leqslant 7$. For $n=2$, tetrahedral NH$_4^-$ may interact with an ammonia molecule by forming a hydrogen bond or an ion-dipole complex. There is also a more stable isomer in which a hydride coordinates to protons from two ammonia molecules. A

hydrogen-bridged species has a $N_2H_7^+$ core with an asymmetric hydrogen bond between the two nitrogen nuclei and two diffuse electrons that are localized outside the three N–H bonds that are vicinal with respect to the bridging proton. In the ion-dipole complex, the three N–H bonds of the ammonia molecule point toward the tetrahedral NH_4^- fragment. The corresponding Dyson orbital for the lowest vertical electron detachment energy strongly resembles that of tetrahedral NH_4^-; there is negligible delocalization onto the ammonia molecule. Assignments of vertical electron detachment energies and vibrational satellites in the photoelectron spectrum were also made with the aid of electron propagator calculations. For $n > 2$, it is likely that low-energy features in more complex spectra may be assigned to double Rydberg anions that exhibit multiple hydrogen bonds or ion-dipole interactions.

Many predictions of double Rydberg anions that are based on elements other than nitrogen have been made on the basis of two necessary conditions: a positive vertical electron detachment energy and a positive definite Hessian matrix (that is, all positive, real harmonic frequencies) at the optimized geometry.[2,3,10–13,17–20] A tetrahedral form of the isoelectronic anion PH_4^-, in addition to a sawhorse isomer that conforms to valence shell electron pair repulsion theory, has been predicted.[13,18–20] A C_{3v} form of OH_3^- was also predicted.[2,3,11–13,17] Dyson orbitals obtained with several self-energy approximations for the lowest vertical detachment energy of the C_{3v} form of OH_3^- are spread chiefly over regions that are outside the three O–H bonds and have low amplitudes near the lone pair of the hydronium (H_3O^+) core.[3,17] The deployment of nodes, symmetry properties, and other features of these Dyson orbitals indicate that the double Rydberg appellation is also appropriate for the C_{3v} form of OH_3^-. A study of NH_3R^- and OH_2R^- anions with $R=CH_3$, NH_2, OH, and F substituents for H concluded that stable double Rydberg forms of $NH_3CH_3^-$, $NH_3NH_2^-$, NH_3OH^-, and $OH_2CH_3^-$ exist.[3]

Despite similar predictions[3,13] of vibrational frequencies and vertical electron detachment energies for C_{3v} OH_3^- and tetrahedral NH_4^-, no experimental observations of double Rydberg anions with nonhydrogen elements other than nitrogen have been made. To guide experimentation on oxygen-based double Rydberg anions, we have performed calculations on C_{3v} OH_3^- and its reaction path to the hydride-water complex. Results on reaction heats and barriers suggest that this double Rydberg anion is a delicate species that may be difficult to prepare and characterize. We therefore examine complexes between this anion and a water molecule that involve hydrogen bonds and ion-dipole forces with possible stabilizing effects. Predictions of structures, vibrational frequencies, relative total energies, and electron binding energies are made on three $O_2H_5^-$ species that exhibit such interactions.

METHODS

Geometry optimizations on minimum structures and harmonic frequency determinations were executed at the QCISD/6-311++G$(2df,2p)$ level.[21,22] Intrinsic reaction
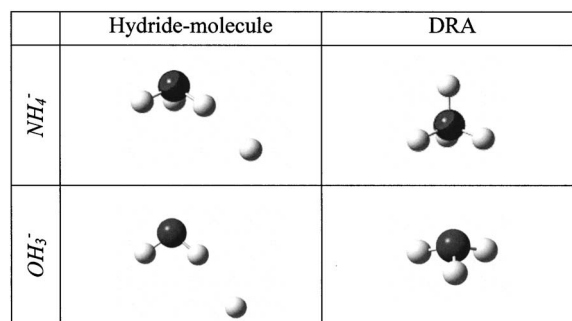

FIG. 1. Hydride-molecule and double Rydberg anion (DRA) structures of NH_4^- and OH_3^-.

coordinate[23] calculations and transition state optimizations were done with the MP2/6-311++G$(2df,2p)$ procedure. Extra diffuse oxygen sp and hydrogen s functions (with exponents that are one-third as large as those in $++$ basis sets) were added in electron propagator calculations of vertical electron detachment energies (VEDEs), pole strengths, and Dyson orbitals. Several diagonal self-energy approximations in the Dyson equation were used: second order, third order, OVGF, and P3.[16,24] These calculations were carried out with GAUSSIAN03.[25] The renormalized, nondiagonal BD-T1 approximation[16,24,26] was also employed. A modified version of GAUSSIAN03 (Ref. [25]) was used in the latter calculations. Dyson orbitals were plotted with contour values of 0.025 using GAUSSVIEW3.09. Analysis of the electron localization function[27] that corresponds to the Hartree-Fock electron density was performed with the TOPMOD (Ref. [28]) program package and with VIS5D (Ref. [29]) for visualization.

RESULTS

OH_3^- and NH_4^- Structures

Figure 1 displays hydride-molecule and double Rydberg anion (DRA) minima for OH_3^- and NH_4^-. These structures agree closely with results of previous reports.[3,15] All hydrogen nuclei are equivalent in the C_{3v} and T_d double Rydberg minima. For the hydride-molecule structures, there are minor distortions of the molecular fragments with respect to the isolated C_{2v} and C_{3v} minima of water and ammonia. Symmetric bonding arrangements in which the hydride anion is equidistant from two or more of the molecules' hydrogen nuclei are transition states.

Hydride elimination pathways for OH_3^- and NH_4^-

The reaction path that connects the $H^-(H_2O)$ and C_{3v} double Rydberg structures of OH_3^- passes through a transition state that lies only 0.22 eV above the latter minimum. Figure 2 shows energy profiles for this pathway and its previously studied counterpart[4] for NH_4^-, where the barrier to dissociation from tetrahedral NH_4^- to $H^-(NH_3)$ is significantly larger, 0.7 eV. In both cases, elongation of a single bond occurs such that a plane (for OH_3^-) or the C_3 axis of symmetry (for NH_4^-) is preserved until the transition state is traversed. In the later stages of each pathway, the emerging hydride anion coordinates to a proton of the product mol-
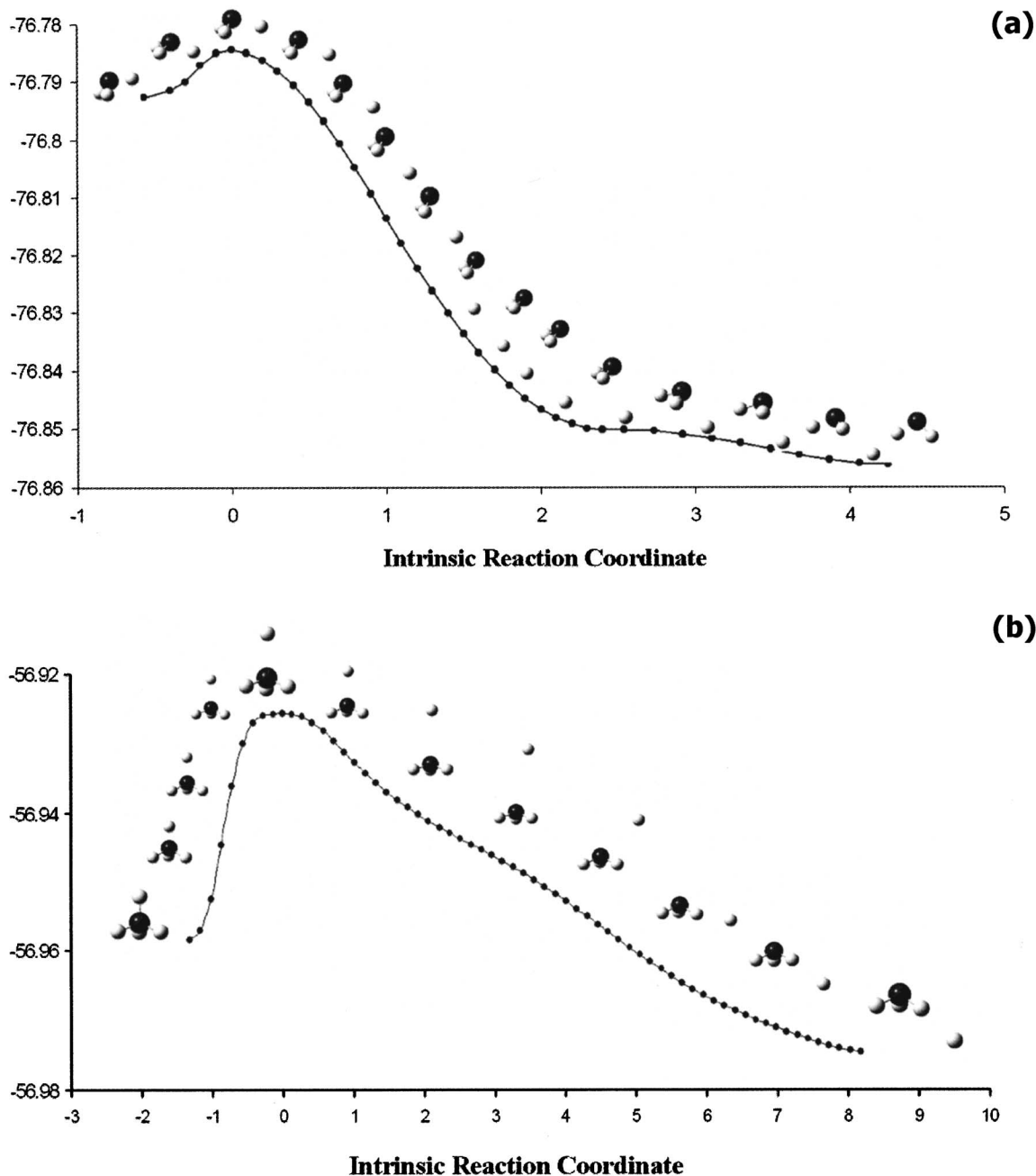
(a)

(b)

FIG. 2. Reaction profiles for hydrogen elimination from (a) OH$_3^-$ and (b) NH$_4^-$. Energy is in au.

ecule. The elimination of H$^-$ from a double Rydberg anion is more exothermic for OH$_3^-$, where $\Delta E = -1.73$ eV, than for NH$_4^-$, where $\Delta E = -0.48$ eV.

To characterize the electronic structure of the geometries that lie along the pathway, VEDEs have been calculated. Table I shows a series of VEDEs and pole strengths p_i, which are defined by

$$p_i = \int |\phi_i^{\mathrm{Dyson}}(x)|^2 dx. \tag{3}$$

(The closer a pole strength comes to unity, the more reliable the diagonal self-energy approximations become.) Because of the decline of some of the pole strengths below 0.8 near the transition state, only the nondiagonal self-energy of the BD-T1 method is a suitable approximation. From the double

Rydberg minimum to the transition state, the VEDE decreases by 0.2 eV. After the transition state, a steady increase of the VEDEs toward the hydride-water limit takes place and pole strengths also become larger. Trends in pole strengths indicate that correlation effects have their greatest qualitative importance near the transition state.

Another characterization tool is provided by the electron localization function (ELF). In Fig. 3, blue, green, and red surfaces represent lone pairs, bond pairs, and Rydberg pairs of electrons, respectively. For the double Rydberg anions (column DRA), the Rydberg electron pair is delocalized and lies outside the bonding regions of the corresponding cationic cores (OH$_3^+$ and NH$_4^+$). There are no lone pairs for NH$_4^-$. In the hydride-molecule column's two structures, each hydride's electrons are sufficiently close to a nearby proton to

TABLE I. VEDEs (eV) along the reaction path of OH_3^-. Pole strengths are in parentheses.

	KT	Second order		Third order		OVGF		P3		BD-T1	
DRA	0.31	0.58	(0.89)	0.46	(0.84)	0.39	(0.76)	0.50	(0.85)	0.50	(0.86)
2	0.33	0.60	(0.88)	0.47	(0.84)	0.40	(0.77)	0.51	(0.84)	0.50	(0.86)
TS	0.39	0.43	(0.83)	0.32	(0.78)	0.29	(0.75)	0.32	(0.79)	0.33	(0.77)
4	0.51	0.01	(0.79)	0.17	(0.75)	0.20	(0.75)	−0.05	(0.78)	0.26	(0.72)
5	0.70	0.10	(0.79)	0.27	(0.81)	0.32	(0.80)	−0.06	(0.83)	0.37	(0.72)
6	0.96	0.13	(0.82)	0.50	(0.85)	0.56	(0.85)	0.18	(0.86)	0.54	(0.75)
7	1.23	0.47	(0.84)	0.76	(0.88)	0.84	(0.87)	0.49	(0.88)	0.76	(0.79)
8	1.49	0.80	(0.86)	1.02	(0.88)	1.11	(0.88)	0.79	(0.89)	1.00	(0.82)
9	1.71	1.08	(0.87)	1.24	(0.89)	1.34	(0.89)	1.04	(0.90)	1.21	(0.83)
10	1.85	1.27	(0.88)	1.39	(0.89)	1.49	(0.89)	1.21	(0.90)	1.36	(0.84)
11	1.91	1.33	(0.88)	1.44	(0.89)	1.49	(0.89)	1.27	(0.90)	1.41	(0.85)
12	1.92	1.35	(0.88)	1.46	(0.89)	1.51	(0.89)	1.29	(0.90)	1.43	(0.85)
13	1.97	1.40	(0.88)	1.54	(0.90)	1.58	(0.90)	1.36	(0.90)	1.50	(0.86)
14	2.05	1.46	(0.89)	1.65	(0.91)	1.71	(0.91)	1.46	(0.91)	1.60	(0.87)
Ionic	2.06	1.47	(0.89)	1.68	(0.91)	1.73	(0.91)	1.48	(0.91)	1.62	(0.87)

be classified as a bond pair. The ELF's assessments of the two transition states differ qualitatively. Whereas the NH_4^- transition state (TS column) has a bond pair basin that resembles the hydride-centered pair of the hydride-ammonia complex, the Rydberg electron pair remains present in the OH_3^- transition state. The latter characterization is compatible with the low-energy barrier and enhanced exothermicity for hydride elimination that is typical of a so-called early transition state. The relatively late transition state of the NH_4^- case bears a stronger resemblance to its anion-molecule product.

$O_2H_5^-$ and $N_2H_7^-$ structures

A comparison of $O_2H_5^-$ and $N_2H_7^-$ minima is shown in Fig. 4. Results for the latter anion are in agreement with those that have been published recently.[15] A hydride anion coordinated to slightly elongated O–H or N–H bonds from two molecules is found in each of the structures of column A. Asymmetric hydrogen bridges connect the nonhydrogen nuclei in the next column. Double Rydberg anions are coordinated to molecules in the minima of column C. Corresponding structures of O_2H_5 and $O_2H_5^+$ are found in the last two rows. Details of the $O_2H_5^-$ structures are listed in Table II. The vibrational frequencies of Table III indicate that all three $O_2H_5^-$ structures are minima, but only the hydrogen-bridged geometry of O_2H_5 has the same property of stability.

The hydrogen-bridged $O_2H_5^-$ structure is about 2.3 eV less stable than the $H^-(H_2O)_2$ minimum. In the former structure, the bridging H_3 nucleus has an elongated distance, 1.05 Å, from O_1 and a separation of 1.47 Å from O_2. This asymmetric geometry resembles that of the corresponding hydrogen-bridged cation, $O_2H_5^+$, which is generally considered to have a hydrogen bond between OH_3^+ and H_2O fragments. A noteworthy difference between the cationic and anionic structures is the reorientation of the H_1 and H_2 nuclei

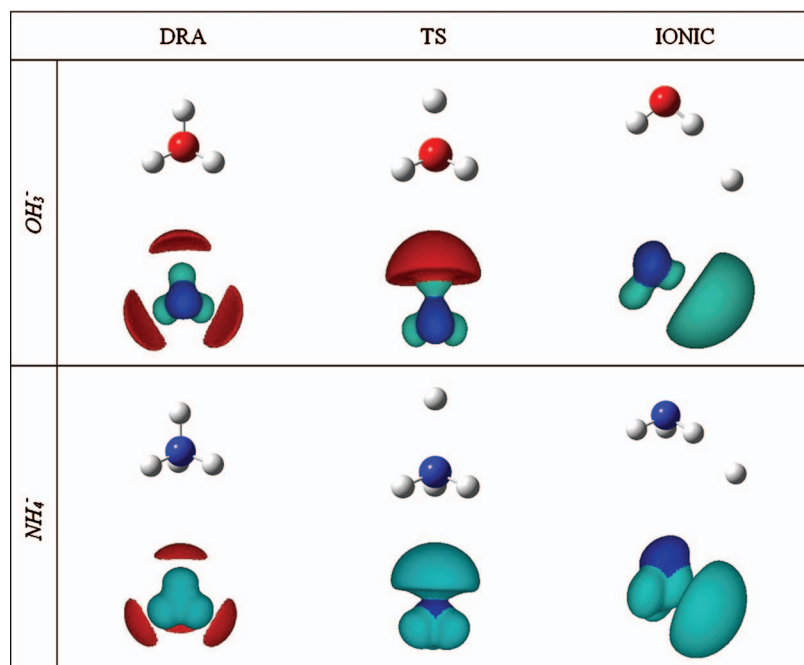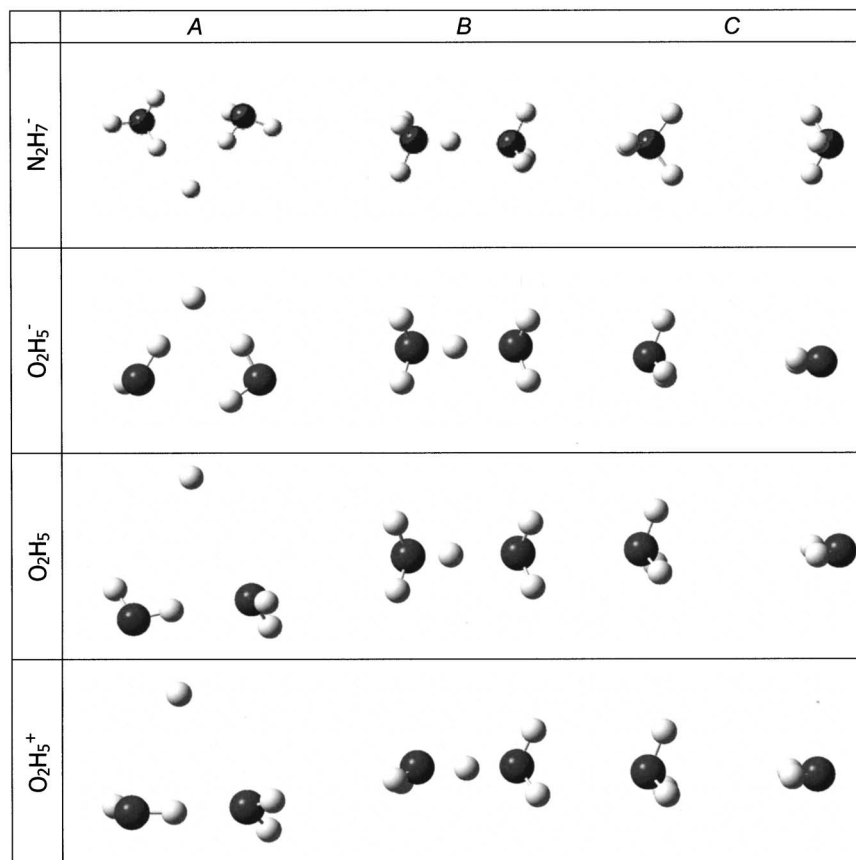
FIG. 3. (Color) ELF analysis of double Rydberg anion (DRA), transition state (TS), and hydride-molecule structures for OH_3^- and NH_4^-.

FIG. 4. Optimized structures for N$_2$H$_7^-$, O$_2$H$_5^-$, O$_2$H$_5$, and O$_2$H$_5^+$.

which is effected by a rotation of the OH$_3$ fragment about the hydrogen-bridge axis. The uncharged radical's structure more closely resembles that of the anion, whereas the OH$_3^-$ fragment forms a hydrogen bridge with the neighboring water molecule in the structure of column B. It orients all three of its hydrogens toward the positive end of the water molecule's dipole moment in column C. This anion-molecule complex is only 0.07 eV less stable than the bridged isomer and has a markedly greater distance between the oxygen nuclei.

O$_2$H$_5^-$ vertical electron detachment energies

For all three O$_2$H$_5^-$ minima, vertical electron detachment energies and corresponding Dyson orbitals are displayed in Table IV. In addition to results obtained with various electron propagator approximations, uncorrelated, frozen-orbital values that are based on Koopmans's theorem (KT) are listed. By far the largest VEDE belongs to the H$^-$(H$_2$O)$_2$ complex. Relaxation and correlation corrections to KT results amount to several tenths of an eV. Pole strengths are

TABLE II. QCISD optimized geometries and total energies for O$_2$H$_5^-$ including Zero-point energy corrections.

Complex A	Complex B	Complex C
d(O$_1$-O$_2$)= 3.11	d(O$_1$-O$_2$)= 2.52	d(O$_1$-O$_2$)= 4.36
d(O$_1$-H$_3$)= 2.54	d(O$_1$-H$_3$)= 1.05	d(O$_1$-H$_3$)= 1.01
d(O$_2$-H$_3$)= 2.67	d(O$_2$-H$_3$)= 1.47	d(O$_2$-H$_3$)= 4.15
d(O$_1$-H$_1$)= 0.96	d(O$_1$-H$_1$)= 1.00 = d(O$_1$-H$_2$)	d(O$_1$-H$_1$)= 1.02 = d(O$_1$-H$_2$)
d(O$_1$-H$_2$)= 1.00	d(O$_2$-H$_4$)= 0.97 = d(O$_2$-H$_5$)	d(O$_2$-H$_4$)= 0.96 = d(O$_2$-H$_5$)
d(O$_2$-H$_4$)= 0.98	H$_1$-O$_1$-H$_2$= 106.3	H$_1$-O$_1$-H$_2$= 106.9
d(O$_2$-H$_5$)= 0.96	H$_4$-O$_2$-H$_5$= 104.5	H$_4$-O$_2$-H$_5$= 101.9
H$_1$-O$_1$-H$_2$= 101.2	O$_1$-H$_3$-O$_2$= 177.9	O$_1$-H$_3$-O$_2$= 95.6
H$_4$-O$_2$-H$_5$= 99.3	H$_1$-O$_1$-H$_3$-O$_2$= -58.5	H$_3$-O$_1$-O$_2$-H$_5$= 89.8
O$_1$-H$_3$-O$_2$= 73.4	O$_1$-H$_3$-O$_2$-H$_5$= 61.2	H$_4$-O$_2$-O$_1$-H$_1$= 29.1
H$_1$-O$_1$-H$_3$-O$_2$= -94.5		
O$_1$-H$_3$-O$_2$-H$_5$= -6.9		
Total Energy = -153.166618au	Total Energy = -153.081481au	Total Energy = -153.08407au

TABLE III. $O_2H_5^-$ and O_2H_5 vibrational frequencies (cm^{-1}).

Complex A	Radical	Anion
ν_1	19.013i	76.804
ν_2	17.872	98.671
ν_3	63.714	388.628
ν_4	127.108	418.386
ν_5	150.676	472.156
Complex B	Radical	Anion
ν_1	19.624	31.198
ν_2	219.828	271.598
ν_3	277.555	355.758
ν_4	354.506	403.516
ν_5	579.211	653.722
Complex C	Radical	Anion
ν_1	57.280i	35.255
ν_2	20.764i	57.639
ν_3	29.246	61.061
ν_4	54.822	90.352
ν_5	70.339	154.350

above 0.9 for the diagonal self-energy (2, 3, OVGF, and P3) approximations and thereby confirm the qualitative validity of the Koopmans description. The most advanced approximation, BD-T1, obtains a VEDE of approximately 2.36 eV, a pole strength of 0.89, and a Dyson orbital localized on the hydride's nucleus that confirms the results of the simpler methods. Given the higher stability of this isomer, a peak near 2.4 eV can be expected to dominate the photoelectron spectrum of $O_2H_5^-$. In the Dyson orbital for the VEDE, only a little delocalization from the hydride anion to the vicinity of O–H bonds occurs.

In the hydrogen-bridged anion, there is fairly close agreement in the VEDE predictions of the propagator methods. The KT prediction is markedly lower. A pole strength of only 0.7 for the OVGF calculation makes the corresponding VEDE prediction unusable. Agreement between the BD-T1 results and those of the other diagonal self-energy methods (2, 3, and P3) is good. The Dyson orbital's amplitudes are largest near the two, nonbridging OH_3^- hydrogens, H_1 and H_2. There is considerable delocalization to regions near the water molecule's protons, H_4 and H_5.

Approximately 0.3 eV separates the predicted VEDEs of the hydrogen-bridged structure and the double Rydberg anion-molecule complex. The more stable of these two isomers has the smaller VEDE. Relaxation and correlation corrections to KT results are also substantial in the $NH_4^-(NH_3)$ species. BD-T1 calculations are in good agreement with second order, third order, and P3 predictions. In the corresponding Dyson orbital, the largest amplitudes occur outside the three O–H bonds of the OH_3^- fragment. There is negligible delocalization onto the coordinated water molecule. This Dyson orbital closely resembles its counterpart for the VEDE of free OH_3^-.
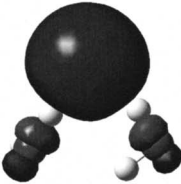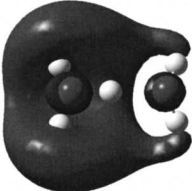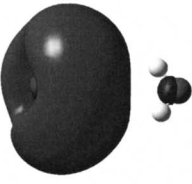
Between the predicted VEDEs of the double Rydberg anion-molecule complex and the hydrogen-bridged double Rydberg anion lies the value that pertains to the OH_3^- double Rydberg anion (see Table I). Coordination of the water molecule increases the VEDE by 0.2 eV. The hydrogen-bridged double Rydberg anion's VEDE differs from that of double Rydberg OH_3^- by a few hundredths of an eV. A similar ordering is obtained for the VEDEs of the $NH_4^-(NH_3)$, NH_4^-, and hydrogen-bridged $N_2H_7^-$ double Rydberg anions.[15]

DISCUSSION

NH_4^- versus OH_3^-

Tetrahedral NH_4^- and C_{3v} OH_3^- are stable minima in their potential energy surfaces and have VEDEs that lie within 0.1 eV of each other. Given the repeated observation and extensive characterization of the former anion, some consideration should be given to the possibility of preparing and spectroscopically interrogating the latter anion. Comparison of the barriers and reaction energies of Fig. 2 shows the reason why OH_3^- may be considerably more difficult to isolate. Relatively small changes in electronic structure accompany the transformation of the OH_3^- double Rydberg anion into a transition state than is seen in the NH_4^- case. To extend the double Rydberg concept to oxygen-containing species, stabilization of C_{3v} OH_3^- by hydrogen bonding or by ion-dipole intermolecular interactions should be considered.

TABLE IV. $O_2H_5^-$ Dyson orbitals and VEDEs (eV). Pole strengths are in parentheses.

	A	B	C
Dyson Orbital			
KT	2.76	0.18	0.47
2nd Order	2.19 (0.90)	0.52 (0.89)	0.78 (0.89)
3rd Order	2.41 (0.91)	0.41 (0.84)	0.68 (0.85)
OVGF	2.17 (0.91)	0.33 (0.71)	0.64 (0.82)
P3	2.17 (0.91)	0.44 (0.85)	0.72 (0.86)
BD-T1	2.36 (0.89)	0.48 (0.86)	0.74 (0.88)

$O_2H_5^-$ versus $N_2H_7^-$

The photoelectron spectrum of $N_2H_7^-$ displays large peaks that may be assigned to electron detachment from the hydride of a $H^-(NH_3)_2$ complex. In addition, at smaller electron binding energies are peaks that have been assigned to a hydrogen-bridged double Rydberg anion and to an ion-molecule complex composed of tetrahedral NH_4^- and an ammonia molecule. All three of these structures have an oxygen-containing analog. As in the nitrogen-containing case, the most stable species has a hydride that is coordinated to two molecules via attractions to their protons. Hydrogen-bridged $O_2H_5^-$ has discernible OH_3^- and H_2O fragments. The same two fragments, bound to each other not by a hydrogen bond but by an anion-dipole interaction, are also present in the least stable species.

The two double Rydberg isomers of $N_2H_7^-$ have VEDEs that bracket that of tetrahedral NH_4^-. The same bracketing takes place for the double Rydberg structures of $O_2H_5^-$ with respect to the predicted OH_3^- VEDE. Dyson orbitals for VEDEs of the hydrogen-bridged $N_2H_7^-$ and $O_2H_5^-$ species are delocalized outside the nonbridging bonds of the double Rydberg anion fragment. For the double Rydberg anion-molecule complexes, the Dyson orbitals are localized on the anion and strongly resemble their counterparts for the free double Rydberg anions. The nearby molecule's dipole moment is chiefly responsible for the increased VEDE of the anion-complex versus that of the isolated double Rydberg anion.

CONCLUSIONS

The C_{3v} double Rydberg anion OH_3^-, despite its robust vibrational frequencies and vertical electron detachment energies, has a smaller barrier and a larger reaction heat for formation of a hydride-molecule complex than does tetrahedral NH_4^-. Therefore, it is probably more difficult to isolate and characterize the former double Rydberg anion than the latter with mass spectrometry and photoelectron spectroscopy. Calculations of vertical electron detachment energies and analysis of the electron localization function disclose that, in contrast to the NH_4^- case, relatively minor changes in electronic structure occur between the double Rydberg anion and the transition state that leads to hydride elimination.

In $O_2H_5^-$, the C_{3v} OH_3^- anion may engage a water molecule through a hydrogen bond or it may form an ion-dipole complex with H_2O. Both of these structures are less stable than a complex which may be represented as $H^-(H_2O)_2$, where a hydride is coordinated to protons from two water molecules. Predictions of the vertical electron detachment energies of these species are 2.36 eV for $H^-(H_2O)_2$, 0.48 eV for hydrogen-bridged $O_2H_5^-$, and 0.74 eV for ion-dipole $OH_3^-(H_2O)$. These values may be compared with 0.50 eV for C_{3v} OH_3^- and 1.62 eV for $H^-(H_2O)$. Electron propagator methods that are comparable in accuracy to those that successfully predicted the VEDEs of the three corresponding $N_2H_7^-$ isomers have been used.

[1] J. T. Snodgrass, J. V. Coe, C. B. Freidhoff, K. M. McHugh, and K. H. Bowen, Faraday Discuss. Chem. Soc. **86**, 241 (1988).

[2] J. Simons and M. Gutowski, Chem. Rev. (Washington, D.C.) **91**, 669 (1991).

[3] H. Hopper, M. Lococo, O. Dolgounitcheva, V. G. Zakrzewski, and J. V. Ortiz, J. Am. Chem. Soc. **122**, 12813 (2000).

[4] J. Melin, G. Seabra, and J. V. Ortiz, in *Theoretical Aspects of Chemical Reactivity*, edited by A. Toro-Labbé (Elsevier, Amsterdam, 2007), pp. 87.

[5] J. T. Snodgrass, Ph.D. dissertation, Johns Hopkins University, 1986.

[6] J. V. Coe, Ph.D. dissertation, Johns Hopkins University, 1986.

[7] H. Cardy, C. Larrieu, and A. Dargelos, Chem. Phys. Lett. **131**, 507 (1986).

[8] D. Cremer and E. Kraka, J. Phys. Chem. **90**, 33 (1986).

[9] J. V. Coe, J. T. Snodgrass, C. B. Freidhoff, K. M. McHugh, and K. H. Bowen, J. Chem. Phys. **83**, 3169 (1985).

[10] J. V. Ortiz, J. Chem. Phys. **87**, 3557 (1987).

[11] M. Gutowski, J. Simons, R. Hernandez, and H. L. Taylor, J. Phys. Chem. **92**, 6179 (1988).

[12] M. Gutowski and J. Simons, J. Chem. Phys. **93**, 3874 (1990).

[13] J. V. Ortiz, J. Phys. Chem. **94**, 4762 (1990).

[14] S. J. Xu, J. M. Niles, J. H. Hendricks, S. A. Lyapustina, and K. H. Bowen, J. Chem. Phys. **117**, 5742 (2002); D. Radisic, S. T. Stokes, and K. H. Bowen, *ibid.* **123**, 11101 (2005).

[15] J. V. Ortiz, J. Chem. Phys. **117**, 5748 (2002).

[16] J. V. Ortiz, Adv. Quantum Chem. **33**, 35 (1999).

[17] J. V. Ortiz, J. Chem. Phys. **91**, 7024 (1989).

[18] N. Matsunaga and M. S. Gordon, J. Phys. Chem. **99**, 12773 (1995).

[19] G. Trinquier, J. P. Daudey, G. Caruana, and Y. Madaule, J. Am. Chem. Soc. **106**, 4794 (1984).

[20] J. Moc and K. Morokuma, Inorg. Chem. **33**, 551 (1994).

[21] J. A. Pople, M. Head-Gordon, and K. Ragavachari, J. Chem. Phys. **87**, 5968 (1987).

[22] R. Krishnan, J. S. Binkley, R. Seeger, and J. A. Pople, J. Chem. Phys. **72**, 650 (1980); M. J. Frisch, J. A. Pople, and J. S. Binkley, *ibid.* **80**, 3265 (1984).

[23] K. Fukui, Acc. Chem. Res. **14**, 363 (1981); C. Gonzalez and H. B. Schlegel, J. Chem. Phys. **90**, 2154 (1989).

[24] J. V. Ortiz, in *Computational Chemistry: Reviews of Current Trends*, edited by J. Leszczynski (World Scientific, Singapore, 1997), Vol. 2.

[25] M. J. Frisch, G. W. Trucks, H. B. Schlegel *et al.*, GAUSSIAN 03 (Gaussian, Inc., Pittsburgh PA, 2003).

[26] J. V. Ortiz, J. Chem. Phys. **109**, 5741 (1998).

[27] A. D. Becke and K. E. Edgecombe, J. Chem. Phys. **92**, 5397 (1990).

[28] S. Noury, X. Krokisdis, F. Fuster, and B. Silvi, Comput. Chem. (Oxford) **23**, 597 (1999).

[29] B. Hibbard, J. Kellum, and B. Paul, VIS 5D, version 5.2, Visualization Project, University of Wisconsin-Madison Space Science and Engineering Center, 1990.